WATER RESOURCES RESEARCH, VOL. 29, NO. 8, PAGES 2599–2613, AUGUST 1993

On the Use of Digital Elevation Model Data for Hortonian and Fractal Analyses of Channel Networks

KEITH R. HELMLINGER, PRAVEEN KUMAR,[1] AND EFI FOUFOULA-GEORGIOU

St. Anthony Falls Hydraulic Laboratory, Department of Civil and Mineral Engineering, University of Minnesota, Minneapolis

A common method of channel network extraction from digital elevation model (DEM) data is based on specification of a threshold area A_{th}, that is, the minimum support area required to drain to a point for a channel to form. Current efforts to predict A_{th} from DEM data are inconclusive, and usually an arbitrary constant A_{th} value is chosen for channel network extraction. In this paper, we study the effects of threshold area selection on the morphometric properties (such as drainage density, length of drainage paths, and external and internal links) and scaling properties (such as Horton's laws and fractal dimension) of a channel network. We also study the related problem of DEM data resolution and its effect on estimation of scaling properties. The results indicate that morphometric properties vary considerably with A_{th}, and thus values reported without their associated A_{th} are meaningless and should be used in hydrologic analysis with caution. Also, the "completeness" of a channel network (in terms of having the outlet stream flowing directly into a higher-order stream) is found to depend on A_{th} in a random unpredictable way. Even if only the complete channel networks are used in the analysis, the statistical variability of scaling properties estimates due to A_{th} selection is significant and can be of comparable size to the variability due to DEM resolution and variability between estimates of different river networks. Our analysis highlights the need to carefully study the problem of network source representation or channel initiation scale from DEMs which will point to an appropriate A_{th} for channel network extraction and estimation of morphometric properties.

1. INTRODUCTION

It has long been recognized that catchment geomorphology relationships can be used as predictors of catchment flood properties. For example, mean channel length is commonly used in empirical formulae predicting the time of concentration of a basin [*Eagleson*, 1970], and the mean annual flood or flood quantiles are often related to the drainage area of the basin or to the drainage density of the river network [*Carlston*, 1963]. Hydraulic distances (along the drainage network) and corresponding travel times from points in the basin to the outlet play an important role in determining the geomorphologic unit hydrograph (GUH) of a basin. In fact, the geomorphologic instantaneous unit hydrograph (GIUH), which is the impulse response of a basin to a unit pulse of precipitation excess, may be viewed as the probability density function (pdf) of travel times to the outlet of water particles injected uniformly in space [*Rodriguez-Iturbe and Valdes*, 1979; *Gupta et al.*, 1980] and can be parameterized in terms of Horton's scaling ratios [e.g., *Rosso*, 1984]. More recently, physically based topographically driven hydrologic models that use topographic features extracted from DEMs have found increased applicability for runoff prediction (for example, see *Quinn et al.* [1991] and the review article of *Moore et al.* [1991, and references therein]).

From the above it is apparent that the practical need arises for accurately defining the drainage paths in a network, that is, for extracting the so-called channel network from the topography or landscape of the basin. Field studies can be used to define the drainage paths in a network, but this is a very tedious, time-consuming, and expensive method which unfortunately becomes impractical in most hydrologic studies. A commonly used alternative is to use topographic maps. However, *Morisawa* [1959] and *Coates* [1958] suggest that the networks obtained from blue lines on U.S. Geological Survey (USGS) topographic maps with scales 1:62,500 and 1:24,000 are generally unreliable. The topographic maps are unable to detect certain first-, second-, and third-order streams, and this produces a network whose order, and number and average length of streams are different from those of the true network. This is nicely illustrated by Figures 1 and 2 of *Coffman et al.* [1972], which indicate that blue line networks from 1:24,000 topographic maps miss almost all first- and second-order true streams, with the true stream orders obtained from field-checked aerial photographs.

Recently, the wide availability and power of computers has stimulated the use of digital elevation models (DEM) for automatic channel network extraction. Digital elevation models are available from the USGS for all of the contiguous United States, Hawaii, and limited portions of Alaska in 1° by 1° blocks with elevations given at a spacing of 3 arc seconds. The resulting grid spacing of these DEMs depends on latitude (for example, in Minnesota it is approximately 65 by 90 m). For some portions of the United States more detailed data are available in 7.5 by 7.5 min blocks which correspond to the USGS topographic quadrangle maps and have elevation data on a regularly spaced grid of 30 by 30 m. Once the DEM data are available, procedures for extracting the channel network and delineating the basins and subbasins exist (see, for example, *O'Callaghan and Mark* [1984], *Jenson* [1987], *Jenson and Domingue* [1988], *Mark* [1988], *Martz and deJong* [1988], *Yuan and Vanderpool* [1986], *Morris and Heerdegen* [1988], *Qian et al.* [1990], *Fairfield and Leymarie* [1991], *Freeman* [1991], *Tribe* [1992], and *Chorowicz et al.* [1992], among others). Although some of

[1]Now at Hydrologic Sciences Branch, Laboratory for Hydrospheric Processes, NASA Goddard Space Flight Center, Greenbelt, Maryland.

Copyright 1993 by the American Geophysical Union.

Paper number 93WR00545.
0043-1397/93/93WR-00545$05.00

the newest algorithms permit multiple flow directions [e.g., *Freeman*, 1990], single flow direction algorithms are still most commonly used. These are usually based on a steepest gradient type of drainage path. That is, water flows along one of eight possible paths (following a square grid discretization) depending on the steepest slope. Pits or points surrounded by neighbors with higher elevations can occur in the DEM data as a result of data errors, sampling effects, and natural features. A "flooding" procedure, where pits are made to drain in the direction that water would overflow from the pit, is often used to determine the flow direction from a pit [e.g., *Mark*, 1988; *Jenson and Domingue*, 1988], although other procedures [e.g., *Band*, 1986; *Seemuller*, 1989; *Chorowicz et al.*, 1992] have been proposed.

An important aspect of any channel network extraction algorithm is to decide where to begin the channels. The most common approach consists of specifying a threshold area A_{th} (usually assumed constant) which is the minimum area required to drain to a point for a channel to form [e.g., *Band*, 1986, 1989; *Jenson and Domingue*, 1988; *Morris and Heerdegen*, 1988; *Lammers and Band*, 1990; *Tarboton et al.*, 1988, 1991; *Gardner et al.*, 1991; *Tribe*, 1991]. This threshold area for channel initiation is usually specified arbitrarily although it is recognized that different threshold areas will result in substantially different channel networks for the same basin. The purpose of this paper is to study the effect of the chosen threshold area on the morphometric properties (such as drainage density, length of drainage paths, statistics of external and internal links) and scaling properties (such as Horton's ratios and fractal dimensions) of a channel network.

Channel network, stream network, river network and drainage network have been used interchangeably in the literature (see *Chorowicz et al.* [1992] for discussion). Here we adopt the terminology of channel or drainage network as more appropriate for the features (that is, channels or permanent features of the basin recognizable even at the absence of flow [*Montgomery and Dietrich*, 1988]) which we try to extract from the DEM data. *Montgomery and Dietrich* [1988] discuss methods of locating channel heads in the field. Field-observed "true" channel networks are needed in order to test and validate theories, as those discussed below, aiming at predicting the channel initiation scale from DEMs.

Tarboton et al. [1989] proposed a method of predicting the channel initiation scale based on the stability threshold of *Smith and Bretherton* [1972] which defined the transition from stable diffusive processes to unstable channel-forming processes. The different scaling behavior in the stable and unstable regimes was shown to be equivalent to a change in the sign of the slope-area scaling function gradient. Thus the area at which a break of slope in a slope-area plot occurred was interpreted as the scale at which stability changes and was then used as A_{th} to define channel initiation. However, in our opinion, the implementation of this method to DEM extracted channel networks has been inconclusive since, as *Tarboton et al.* [1989, p. 202] point out, "the slope-area scaling break was usually just a steepening of a negative slope and not a change from positive to negative slope as required by the theoretical stability analysis." *Helmlinger and Foufoula-Georgiou* [1992] investigated the possibility of inferring the length scale of transition from hillslope to channel processes based on the hypothesis that scaling laws, for which there is evidence at the channel scale [e.g., *Tarboton et al.*, 1988; *LaBarbera and Rosso*, 1989], would break down below a characteristic critical support area. This break in scaling laws would occur since the mechanisms of runoff production and distribution and sediment transport are expected to be different at the hillslope and channel scales. Both the scaling of individual channels and channel networks and scaling of the three-dimensional elevation surfaces [e.g., *Klinkenberg and Goodchild*, 1992; *Mark and Aronson*, 1984] were examined. The results were not conclusive as no clear break in the slopes of the fractal plots was found, at least for the networks analyzed. Data of resolution finer than 30 by 30 m may be needed to detect a break in the scaling laws at the two different scaling regimes.

Recent evidence by *Montgomery and Dietrich* [1992] has suggested that the threshold area (critical support area) is not constant in a basin but is a function of the local valley slope (the slope immediately upstream of the channel source in the unchanneled valley) and therefore may vary within a basin. Based on extensive field studies, their research has identified an empirical relationship (power law) between threshold area and slope (that is, $A_{th} = CS^{-\theta}$ where C and θ are constants empirically determined from field data and S is the local valley slope). This relationship indicates that the greater the local valley slope, the smaller the threshold area defining the initiation of a channel, as is generally observed. Determination of the parameters of this relationship is very tedious and is based on field studies. Efforts are under way to find methods of predicting the parameters of the (A_{th}, S) relationship from morphometric and/or soil-climatic properties of the river basin [*Helmlinger et al.*, 1992; *Montgomery and Foufoula-Georgiou*, 1993.]

Until the problem of channel initiation scale is resolved most researchers and/or practitioners will continue to use an arbitrarily chosen "reasonable" threshold area to extract channel networks from DEMs. Many times blue lines are used as a guidance [e.g., *Andah et al.*, 1987; *Robert and Roy*, 1990; *LaBarbera and Rosso*, 1990] although as discussed earlier this may not be an appropriate choice. Despite this arbitrary selection, when morphometric properties of DEM-extracted channel networks are reported in the literature the threshold area or other details of the channel network extraction procedure are not always reported. In this paper we report the results of a study of the effects of the threshold area on the morphometric properties and scaling properties of the river basin. Although it is expected that morphometric properties will be considerably affected by the selected threshold area (for example, larger channel lengths will be found for smaller threshold areas), scaling properties should not be affected in an ideal Hortonian network. However, actual channel networks are not ideal Hortonian systems. Our analysis shows that estimates of Horton's ratios are significantly affected by the threshold area used for channel network extraction. If one sees these deviations as statistical variability, then our study indicates that the variability of fractal estimates (based on Horton's ratios) due to threshold area selection for the same channel network can be of comparable magnitude to that reported in the literature for different channel networks, that is, networks in different basins. It is very important that all these problems are recognized when estimation of scaling properties is based on DEM data. Another related problem is that of DEM data resolution and its effect on channel network analysis. Other authors have studied the effect of DEM data resolution on

the performance of multiple flow versus single flow direction algorithms [e.g., *Quinn et al.*, 1991], identification of channel initiation scale [e.g., *Tarboton et al.*, 1991], and estimation of topographic index curves driving hydrologic models [e.g., *Quinn et al.*, 1991]. In this paper we give a preliminary account of the effect of DEM data resolution on estimation of scaling properties.

2. Effects of Threshold Area on Morphometric Properties

The DEM data used in this research are in the form of the USGS 7.5 by 7.5 min blocks. These data consist of a regular array of elevations referenced horizontally in the Universal Transverse Mercator (UTM) coordinate system where the reference datum is the North American Datum of 1927 [*U.S. Geological Survey*, 1987]. The data are stored as profiles (ordered from east to west) in which the spacing of the elevations along and between each profile is 30 m. The USGS has used four procedures to collect the digital elevation data for production of the 7.5-min DEMs: (1) the Gestalt Photo Mapper II, (2) manual profiling from photogrammetric stereomodels, (3) stereomodel digitizing of contours, and (4) derivation from digital line graph (DLG) hypsography and hydrography categories. The accuracy of a DEM is dependent on the spatial resolution, quality of the source data, collection and processing procedures, and digitizing systems. Three levels of quality are used to classify each DEM. Virtually all of the 7.5-min DEMs are considered to be of level 1 quality with typical root-mean-square error (rmse) of either 7 or 15 m. The computation of the rmse uses linear-interpolated elevations in the DEM and corresponding "true" elevations from published maps.

Three watersheds, one located in northern California, a second in southeast New York state, and the third in northern Idaho, were extensively studied using the 30-m resolution data. The South Fork Smith River watershed in California (600.4 km^2 at the chosen outlet point) is contained within the Gasquet, Hurdygurdy Butte, Devils Punchbowl, Cant Hook Mountain, Ship Mountain, Prescott Mountain, Klamath Glen, Summit Valley, and Chimney Rock 7.5-min quadrangle maps. The Schoharie Creek watershed in New York (113.6 km^2 at the chosen outlet point) is contained within the Hunter and Kaaterskill 7.5-min quadrangle maps. The Big Creek watershed in Idaho (146.9 km^2 at the chosen outlet point) is contained within the Masonia, Polaris Peak, Calder, and Marble Creek 7.5-min quadrangle maps. Contour maps of the three watersheds are shown in Figures 1*a*, 2*a*, and 3*a*. The method described by *Tarboton et al.* [1988] (based on the work of *Band* [1986] and *O'Callaghan and Mark* [1984]) was used to extract the channel networks. This method uses a constant threshold area to delineate the sources of the order 1 streams. Sample channel networks for these three basins extracted from 30 by 30 m DEM data using threshold areas of 0.4608 km^2 for the South Fork Smith River, 0.6912 km^2 for Schoharie Creek, and 0.2304 km^2 for Big Creek are shown in Figures 1*b*, 2*b*, and 3*b*, respectively.

Drainage network characteristics determined by varying the threshold area are summarized in Table 1 for all three watersheds. Here *Strahler*'s [1952] ordering scheme is used, and streams are defined as segments of the channel network which are composed of continuous links of the same order.

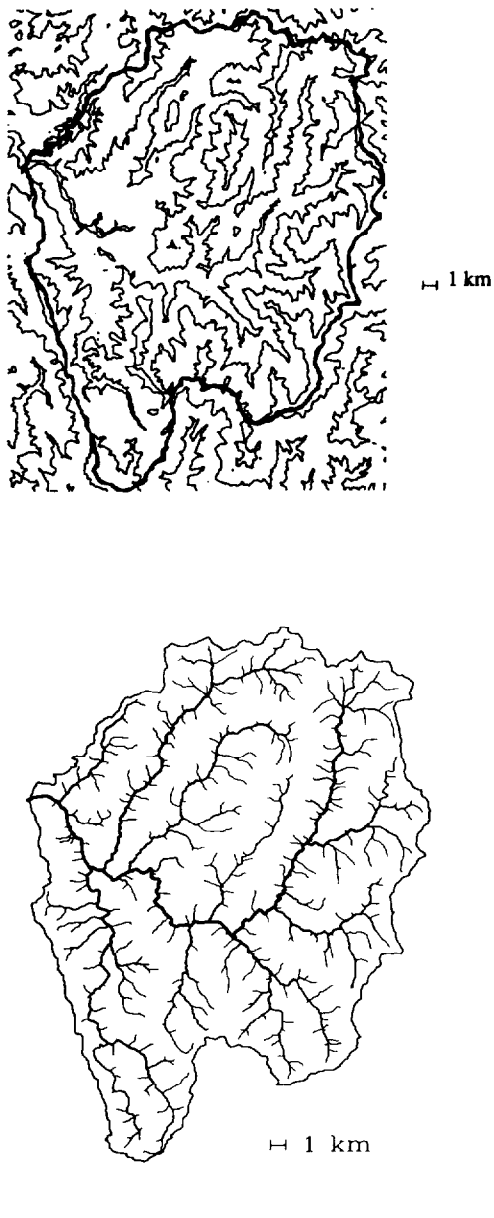

Fig. 1. South Fork Smith River, California, watershed (drainage area, 600.4 km^2). (*a*) Contour map with a minimum contour of 200 m and contour intervals of 400 m. The elevations within the basin range from 134 m (at the outlet) to 1908 m. (*b*) Channel network extracted from 30-m resolution DEM data (threshold area, 0.4608 km^2; network order 5). The streams are drawn so that line thickness is proportional to stream order.

The range of threshold areas studied is arbitrary but covers all "reasonable" threshold areas if one considers that the "blue lines" on the USGS 7.5 by 7.5 min quadrangle maps are approximately somewhere between the threshold areas of 0.2304 and 0.4608 km^2 for the South Fork Smith River, between 0.4608 and 0.9216 km^2 for Schoharie Creek, and between 0.1152 and 0.2304 km^2 for Big Creek. It is seen from Table 1, for example, that as the threshold area increases from 0.0576 km^2 (64 pixels, where one pixel is defined by the DEM resolution, 30 by 30 m here) to 0.9216 km^2 (1024 pixels) for the South Fork Smith River the total stream length decreases from 1578.79 to 406.59 km, the drainage density, whose inverse is considered a characteristic scale of

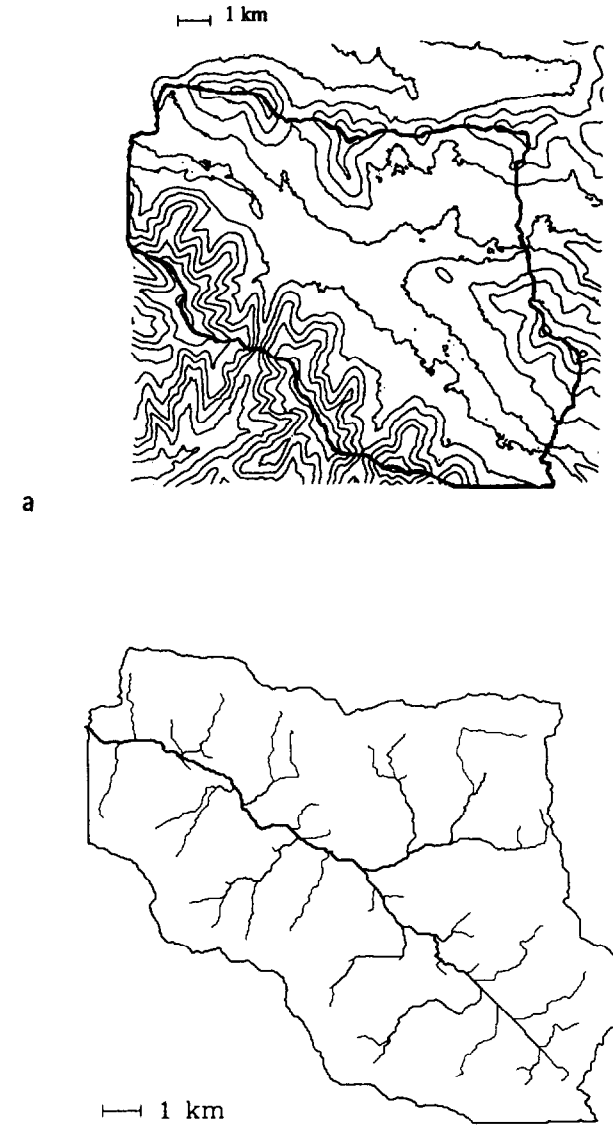

Fig. 2. Schoharie Creek, New York, watershed (drainage area, 113.6 km^2). (*a*) Contour map with a minimum contour of 500 m and contour intervals of 100 m. The elevations within the basin range from 462 m (at the outlet) to 1230 m. (*b*) Channel network extracted from 30-m resolution DEM data (threshold area, 0.6912 km^2; network order 4). The streams are drawn so that line thickness is proportional to stream order.

a landscape, decreases from 2.63 to 0.68 km/km^2, while the mean length of the order 1 streams ($\langle L_1 \rangle$) increases from 0.30 to 1.24 km. In fact, most of these properties, e.g., total number of streams, total stream length, drainage density, and stream frequency, vary linearly with A_{th} in a log-log plot (for example, see Figure 4) suggesting power law relationships. The power law relationship of drainage density with A_{th} has been suggested before [e.g., *Montgomery and Dietrich*, 1989; *Tarboton et al.*, 1991]. While these systematic variations are interesting to know and can be used as predictive tools to obtain properties at one A_{th} from properties of channel networks at another A_{th} they seem to offer no help in pointing out the most appropriate A_{th}.

Table 1 also shows that the length of the outlet stream (L_Ω, where Ω is the order of the basin) can be changed drastically when certain threshold areas are used to define the network. For example, L_Ω for the South Fork Smith River network is 33.13 km for all except two A_{th} areas for which it becomes 7.58 km. For the Big Creek network, L_Ω varies randomly between the values of 12.75, 4.64 and 17.39 km. These drastic changes in the length of L_Ω are the result of removing several key order 1 streams and then having the resulting reduction in order of other streams propagate downstream through the network. The practical implication of this is that the "completeness" of a channel network depends on A_{th} in an unpredictable way. (A "complete" channel network is defined as a network whose outlet point has been selected such that the outlet channel flows imme-

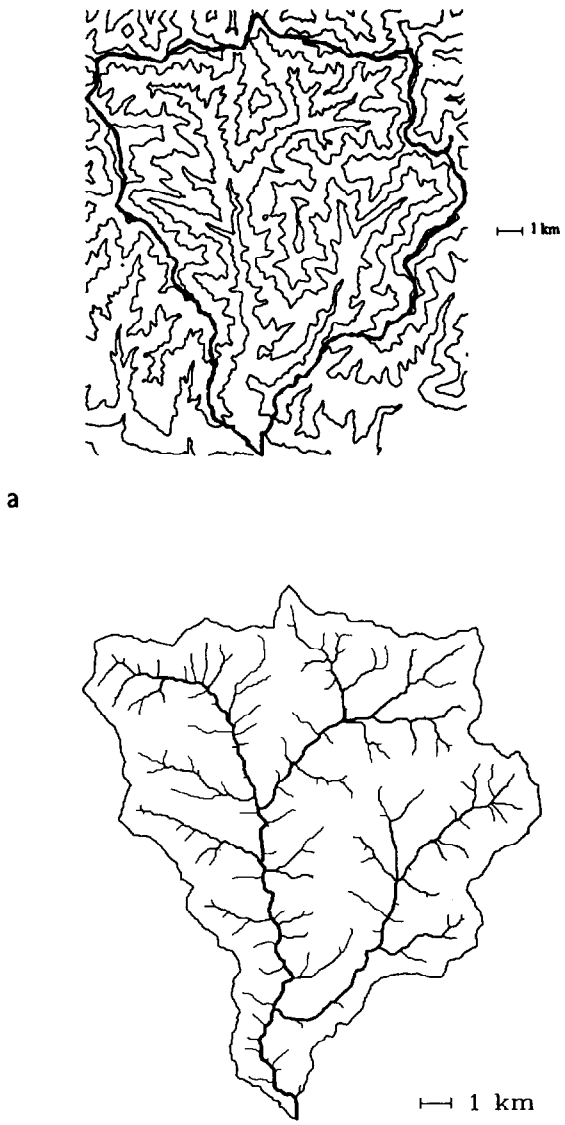

Fig. 3. Big Creek watershed (drainage area, 146.9 km^2). (*a*) Contour map with a minimum contour of 700 m and contour intervals of 200 m. The elevations within the basin range from 682 m (at the outlet) to 1786 m. (*b*) Channel network extracted from 30-m resolution DEM data (threshold area, 0.2304 km^2; network order 5). The streams are drawn so that line thickness is proportional to stream order.

TABLE 1. Effect of Varying Threshold Area on the Network Characteristics From a 30-m Resolution DEM

Threshold Area		Basin							
Area, km^2	Number of Pixels	Order (Ω)	Number of Streams	$\langle L_1 \rangle$, km	L_Ω, km	Total Stream Length, km	Drainage Density, km/km^2	Constant of Channel Maintenance, km^2/km	Stream Frequency, Streams/km^2
				South Fork Smith River, California					
0.0576	64	6	3466	0.30	33.13	1578.79	2.63	0.38	5.77
0.1152	128	6	1690	0.44	33.13	1111.44	1.85	0.54	2.81
0.2304	256	6	834	0.63	7.58	797.73	1.33	0.75	1.39
0.3456	384	5	557	0.77	33.13	662.47	1.10	0.91	0.93
0.4032	448	5	479	0.80	33.13	614.70	1.02	0.98	0.80
0.4608	512	5	425	0.83	33.13	578.81	0.96	1.04	0.71
0.6912	768	5	298	0.98	33.13	471.91	0.79	1.27	0.50
0.9216	1024	5	204	1.24	7.58	406.59	0.68	1.48	0.34
				Schoharie Creek, New York					
0.0288	32	6	1555	0.26	9.55	548.62	4.83	0.21	13.7
0.0576	64	6	786	0.32	9.55	367.35	3.23	0.31	6.92
0.1152	128	5	403	0.39	9.55	239.85	2.11	0.47	3.55
0.2304	256	5	180	0.62	9.55	165.17	1.45	0.69	1.58
0.4608	512	4	90	1.01	9.55	120.71	1.06	0.94	0.79
0.6912	768	4	62	1.16	9.55	96.25	0.84	1.18	0.55
0.9216	1024	4	47	1.43	9.55	84.55	0.74	1.34	0.41
				Big Creek, Idaho					
0.0288	32	6	1791	0.19	12.75	506.22	3.45	0.29	12.2
0.0576	64	6	840	0.26	4.64	344.40	2.34	0.43	5.72
0.1152	128	5	419	0.35	12.75	246.58	1.68	0.60	2.85
0.2304	256	5	224	0.47	12.75	180.69	1.23	0.81	1.53
0.4608	512	4	109	0.82	17.39	135.66	0.92	1.08	0.74
0.6912	768	4	76	1.00	12.75	116.28	0.79	1.26	0.52
0.9216	1024	4	64	1.00	12.75	100.59	0.68	1.46	0.44

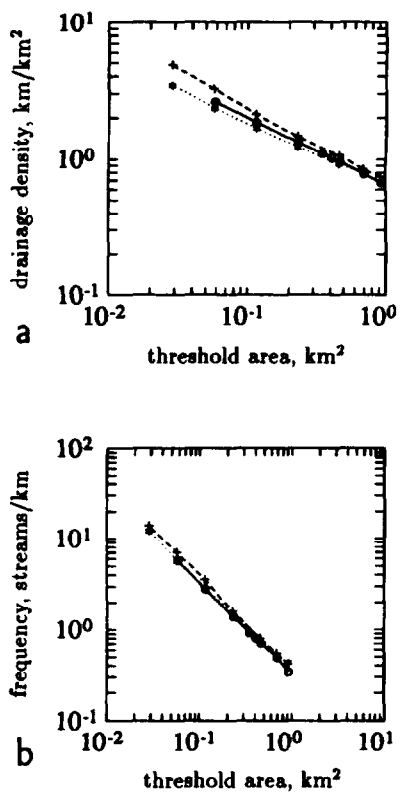

Fig. 4. Variation of (*a*) drainage density and (*b*) stream frequency with threshold area. The solid line is for South Fork Smith River, the dashed line for Schoharie Creek, and the dotted line for Big Creek.

diately into a higher-order channel.) Thus, having selected the outlet point so that the channel network is complete when extracted with one A_{th} does not guarantee that the network obtained with another A_{th} will also be complete. Although it is clear that this is an "artificial" problem caused by the channel network extraction algorithm and the resolution and possibly accuracy of the digital elevation data, it is just one example of the problems that one may encounter when geomorphological relationships are extracted from DEM data. Although it is beyond the scope of this paper to dwell on the DEM data accuracy and appropriateness of the channel network extraction algorithms, this example warns that caution must be exercised in interpreting the results obtained from DEM data. As was well pointed out by *Coffman et al.* [1972, p. 1499], "if stream segments are randomly deleted from a nonrandom network, an apparently random network may be obtained . . . ," and so caution must be exercised to ensure these effects are not the result of data collection or processing procedures.

Table 2 illustrates how the number of streams, the mean stream length, and the mean drainage area vary with stream order for the three networks. The results are reported for two threshold areas for each network, selected such that the blue line networks are somewhere between the networks extracted using these threshold areas. Table 2 shows that for South Fork Smith River at the threshold area of 0.2304 km^2 the length of the order 6 stream is much shorter than the order 5 stream. As discussed above, this corresponds with the removal of several key order 1 streams at this threshold area which results in an incomplete channel network.

TABLE 2. Sample Network Characteristics for Networks Extracted From a 30-m Resolution DEM

Threshold Area, km^2	Stream Order (ω)	Number of Streams	Mean Length, km	Mean Drainage Area, km^2
	South Fork Smith River, California			
0.2304	1	666	0.63	0.55
0.2304	2	132	1.33	2.44
0.2304	3	24	4.07	14.7
0.2304	4	9	5.61	41.3
0.2304	5	2	22.3	278.8
0.2304	6	1	7.58	600.4
0.4608	1	346	0.83	1.02
0.4608	2	58	2.39	5.55
0.4608	3	15	4.90	25.9
0.4608	4	5	9.03	68.4
0.4608	5	1	33.1	600.4
	Schoharie Creek, New York			
0.4608	1	71	1.01	1.10
0.4608	2	16	1.72	4.67
0.4608	3	2	5.86	33.67
0.4608	4	1	9.55	113.6
0.6912	1	48	1.16	1.55
0.6912	2	11	2.12	7.14
0.6912	3	2	3.89	33.67
0.6912	4	1	9.55	113.6
	Big Creek, Idaho			
0.1152	1	327	0.35	0.26
0.1152	2	71	0.92	1.20
0.1152	3	16	1.98	5.46
0.1152	4	4	5.34	28.92
0.1152	5	1	12.75	146.9
0.2304	1	170	0.47	0.50
0.2304	2	40	1.24	2.13
0.2304	3	10	1.83	6.84
0.2304	4	3	6.57	35.97
0.2304	5	1	12.75	146.9

Figures 5*a*–5*c* show the effects of threshold area on several properties of external and internal links for the South Fork Smith River. The properties reported are the mean length $\langle l_e \rangle$ or $\langle l_i \rangle$, drainage area $\langle a_e \rangle$ or $\langle a_i \rangle$ (i.e., area draining directly to the downstream end of an external link and the difference in the areas draining to the downstream and upstream ends of an internal link), and slope $\langle s_e \rangle$ or $\langle s_i \rangle$ (defined as the difference of elevation between the higher and lower elevation point of the link divided by the link length). In Figure 5*d* the dimensionless "microscopic" drainage density $\phi_e = \langle l_e^2/a_e \rangle$ or $\phi_i = \langle l_i^2/a_i \rangle$, defined as the mean of the ratios of the squared link lengths to their associated direct drainage areas [*Smart*, 1972], is shown. Figures 6 and 7 show the same quantities for Schoharie Creek and Big Creek, respectively. These figures illustrate some interesting patterns in the variation of link properties with A_{th}. For example, the mean external and internal link lengths for the South Fork Smith River and Big Creek follow each other closely (Figures 5*a* and 7*a*) while the two curves coincide for only part of the range of threshold areas for Schoharie Creek (Figure 6*a*). Although it is beyond the scope of this paper to interpret these patterns we believe that they hold promise in statistically identifying the appropriate A_{th} from DEM data and also in pointing out cases where a slope-dependent threshold may be more appropriate for watersheds with uneven distribution of slopes, such as Schoharie Creek. Notice from Figure 2*a* that the Schoharie Creek basin has steep slopes in the lower left portion of the basin while the upper right portion is relatively flat with smaller slopes. More supporting evidence for this argument is provided later based on observed irregularities in fractal dimension estimates for this channel network. Within the scope of this paper though, the only point we want to stress is that the effect of threshold area on estimation of morpho-

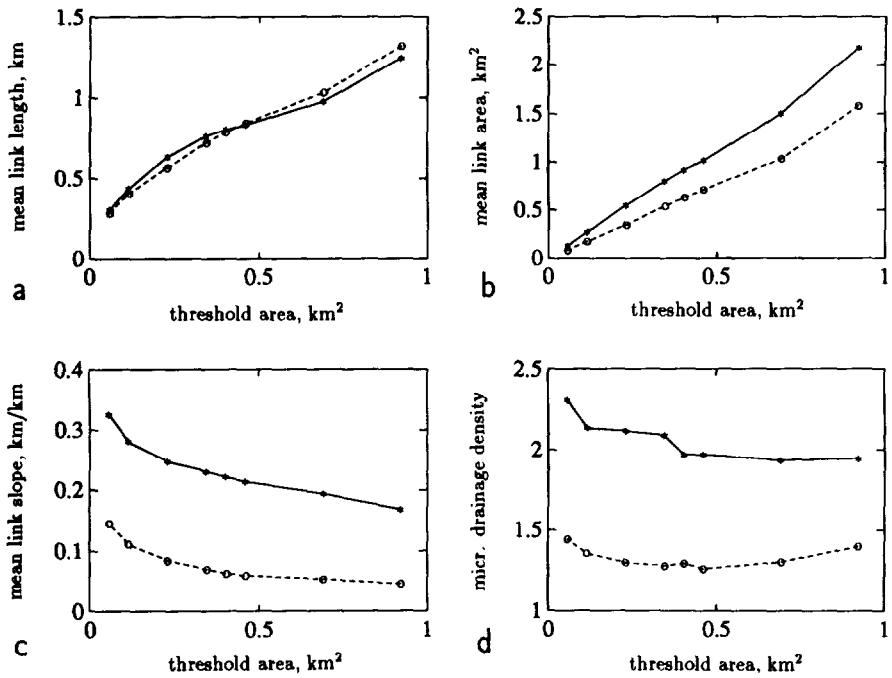

Fig. 5. Effects of threshold area on properties derived from the external (solid line) and internal (dashed line) links of the extracted network for the South Fork Smith River: (*a*) mean link length, $\langle l_e \rangle$ or $\langle l_i \rangle$, (*b*) mean link area, $\langle a_e \rangle$ or $\langle a_i \rangle$, (*c*) mean link slope, $\langle s_e \rangle$ or $\langle s_i \rangle$, and (*d*) mean microscopic drainage density, $\langle l_e^2/a_e \rangle$ or $\langle l_i^2/a_i \rangle$. All terms have been defined in text.

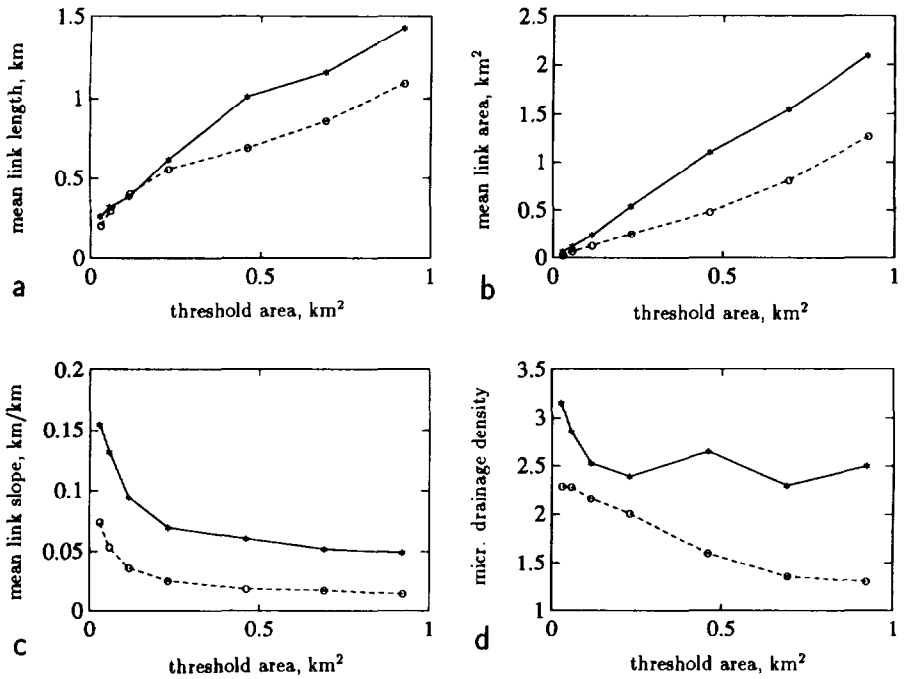

Fig. 6. Same as Figure 5 for Schoharie Creek.

metric properties of the channel network is so significant that reporting these properties without the associated threshold area used to extract the channel network makes their use in hydrologic studies questionable.

3. Effects of Threshold Area on Horton's Ratios and Fractal Dimension

Several authors have recently examined scaling properties of channel networks by looking at the fractality of individual streams and channel networks as a whole [e.g., *Hjelmfelt*, 1988; *Tarboton et al.*, 1988; *LaBarbera and Rosso*, 1989; *Robert and Roy*, 1990; *Rosso et al.*, 1991; *Marani et al.*, 1991]. The fractal dimension of channel networks can be estimated either from Horton's parameters or by a direct method such as box counting. In this section we examine the following issues: (1) sensitivity of Horton's ratios and channel network fractal dimension estimates to the threshold area used for channel network extraction; (2) sensitivity of the box-counting fractal dimension estimates to the threshold area and interpretation of asymptotic results from low-order networks; and (3) comparison of fractal dimension estimates based on Horton's ratios to the box-counting estimates.

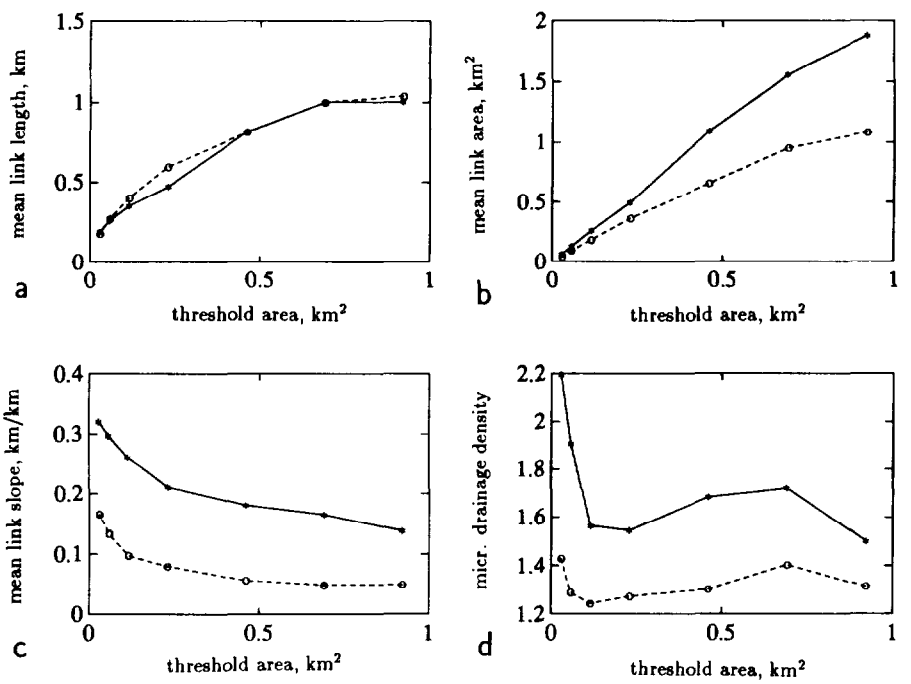

Fig. 7. Same as Figure 5 for Big Creek.

TABLE 3. Horton's Ratios for Networks Extracted From a 30-m Resolution DEM

Threshold Area		Basin			
Area, km^2	Number of Pixels	Order (Ω)	R_B	R_L	log R_B/ log R_L
		South Fork Smith River, California			
0.0576	64	6	4.77 (−0.999)	2.37 (0.999)	1.81
0.1152	128	6	4.37 (−0.999)	2.23 (0.999)	1.84
0.2304	256	6	4.22 (−0.998)	2.08 (0.987)	1.96
			4.22 (−0.998)*	2.29 (0.996)	1.73
0.3456	384	5	4.56 (−0.999)	2.40 (0.999)	1.73
0.4032	448	5	4.41 (−0.998)	2.36 (0.998)	1.73
0.4608	512	5	4.40 (−0.998)	2.39 (0.997)	1.71
0.6912	768	5	4.02 (−0.999)	2.21 (0.993)	1.76
0.9216	1024	5	3.91 (−0.998)	2.03 (0.967)	1.92
			3.91 (−0.998)*	2.45 (0.998)	1.52
		Schoharie Creek, New York			
0.0288	32	6	4.36 (−0.999)	1.98 (0.998)	2.15
0.0576	64	6	4.17 (−0.999)	1.92 (0.987)	2.19
0.1152	128	5	4.41 (−0.998)	2.28 (0.998)	1.80
0.2304	256	5	3.95 (−0.996)	1.89 (0.987)	2.15
0.4608	512	4	4.67 (−0.996)	2.15 (0.990)	2.02
0.6912	768	4	4.06 (−0.996)	1.94 (0.998)	2.11
0.9216	1024	4	3.51 (−0.996)	1.77 (0.977)	2.21
		Big Creek, Idaho			
0.0288	32	6	4.38 (−0.999)	2.21 (0.999)	1.86
0.0576	64	6	4.15 (−0.999)	2.16 (0.993)	1.85
			4.15 (−0.999)*	2.33 (0.998)	1.68
0.1152	128	5	4.37 (−0.999)	2.44 (0.999)	1.65
0.2304	256	5	3.82 (−0.999)	2.25 (0.995)	1.65
0.4608	512	4	4.22 (−0.999)	2.46 (0.988)	1.60
			4.22 (−0.999)*	2.16 (0.987)	1.87
0.6912	768	4	4.08 (−0.999)	2.37 (0.992)	1.63
0.9216	1024	4	3.79 (−0.999)	2.36 (0.986)	1.55

Values in parentheses are the coefficients of correlation R of the weighted least squares regression.

*Row gives estimates where the highest-order stream was omitted.

3.1. *Fractal Dimension Estimates Based on Horton's Ratios*

LaBarbera and Rosso [1987, 1989] derived an expression for the fractal dimension of channel networks as a function of Horton's bifurcation (R_B) and length (R_L) ratios under the assumption that R_B and R_L remain constant within a basin and are independent of scale. Using estimates of R_B and R_L from several basins, *LaBarbera and Rosso* [1989] estimated the fractal dimension of channel networks to be between 1.5 and 2 with an average value between 1.6 and 1.7, which is far from the space-filling value of 2 suggested by the direct (box counting) estimation method of *Tarboton et al.* [1988]. This discrepancy was attributed by *Tarboton et al.* [1990] to the fact that the expression for the fractal dimension of channel networks as derived by *LaBarbera and Rosso* [1989] includes only the effects of the bifurcating structure and not the possible fractality of the individual streams whereas a direct method of estimation includes both effects.

Efforts were made to combine analytically the effects of the fractality of the branching structure with the fractality of the individual streams and obtain an overall fractal dimension for the channel network. Let us call D_s the fractal dimension of the streams, D_b the fractal dimension of the branching structure, and D_{cn} the fractal dimension of the channel network as a whole. *Tarboton et al.* [1990] derived the expression

$$D_{cn} = D_s D_b \tag{1}$$

where D_b was as initially derived by *LaBarbera and Rosso* [1989],

$$D_b = \log R_B / \log R_L \tag{2}$$

while *LaBarbera and Rosso* [1990] derived a different expression based on slightly different assumptions,

$$D_{cn} = D_b/(2 - D_s) \tag{3}$$

Both expressions are practically equivalent for values of D_s close to unity.

Horton's ratios (R_B, R_L, and R_A) are usually estimated by regression techniques from data such as those shown in Table 2. Estimates of Horton's ratios are shown in Table 3 for the South Fork Smith River, Schoharie Creek, and Big Creek where weighted least squares with weights proportional to the number of streams for each order were used. For the threshold areas for which the channel networks were incomplete the results with the highest-order stream removed are also given. If one considers all estimates of R_B and R_L for the complete networks (which would be appropriate given that the worst correlation R in the regression is 0.993 for the South Fork Smith River, 0.977 for Schoharie Creek, and 0.986 for Big Creek) it is observed that the range of log R_B/log R_L is 1.52–1.84 for the South Fork Smith River, 1.8–2.0 for Schoharie Creek (estimates of fractal dimension greater than 2 are taken as 2), and 1.55–1.87 for Big Creek. For Schoharie Creek the fractal dimension estimates are greater than 2 for all except one A_{th} area. An explanation of this is offered later in section 3.

It should be noted that the weighted least squares procedure is considered to be more appropriate than ordinary least squares for estimation of Horton's ratios because there is a great difference in the number of streams of each order in the network (see Table 2). While ordinary least squares give equal weights to the property (such as mean stream length, etc.) for each stream order, the weighted least squares essentially ignore the values from the higher-order streams. As is seen in Table 2 most of the weight is given to the order 1 and 2 streams, which also results in the high correlation coefficients. For comparison purposes, if ordinary least squares are used the range of log R_B/log R_L estimates is 1.61–1.70 for the South Fork Smith River, 1.86–2.00 for Schoharie Creek, and 1.44–1.70 for Big Creek [see *Helmlinger and Foufoula-Georgiou*, 1992].

From the above analysis it is observed that the threshold area used for channel network extraction affects the estimation of Horton's parameters and fractal dimension. If the variability of these estimates is considered as natural variability (as it would be in most studies given the large R values), then the range of fractal dimension estimates is significant (a range of 0.2–0.3), rendering these estimates unreliable for practical purposes. It is emphasized that the derivation of fractal dimension as a function of Horton's ratios, i.e., log R_B/log R_L, assumes that Horton's laws hold perfectly and that Horton's ratios are constant within the basin. Statistically speaking, the high values of R in the regressions imply that Horton's laws hold satisfactorily and that most of the reported fractal dimension estimates are statistically acceptable.

3.2. *Box Counting Estimates of Fractal Dimension*

Falconer [1990, p. 38] gives a widely used definition of the box-counting dimension of a curve as follows. Draw a mesh of squares or boxes of side ε and count the number of boxes $N(\varepsilon)$ that overlap the curve for various small ε. The box-counting dimension is the logarithmic rate at which $N(\varepsilon)$ increases as $\varepsilon \to 0$ and may be estimated from the slope of the graph of log $N(\varepsilon)$ versus log ε. The box-counting dimension is given by

$$D_{\text{box}} = \lim_{\varepsilon \to 0} \frac{\log N(\varepsilon)}{-\log \varepsilon} \tag{4}$$

The number of squares of side ε that intersect the curve is an indication of how irregular the curve is when examined at scale ε. The dimension reflects how rapidly the irregularities develop as $\varepsilon \to 0$ and will range between 1 and 2 for a curve.

Tarboton et al. [1988] used the box-counting method to estimate the fractal dimension of channel networks. Their results indicated two straight lines on the log-log fractal plot: one line at small ε (that is, small box sizes) with slope close to 1 and another line at large ε with slope close to 2. The first line was interpreted as giving the fractal dimension of individual streams and the second line as giving the fractal dimension of the channel networks which indicated that networks are space filling. Of course, the true fractal dimensions of these channel networks were not known so the performance of the box-counting method and the validity of these interpretations could not be verified (except by comparison with the results obtained by some other methods). In this section we first examine the performance and interpretation of the box-counting method plots by applying the method on generated fractal trees of known fractal dimension. To separate the effects of the fractality of the branching structure and the individual streams, we have generated fractal trees which have links as straight lines (that is, D_s = 1 and, therefore, $D_{cn} = D_b$). We then apply the box-counting estimation method to actual channel networks.

3.2.1. *Artificial channel networks.* A fractal tree (that is, an artificial channel network) can be generated by a hyperbolic iterated function system (IFS) with condensation [*Barnsley*, 1988] using either a deterministic algorithm or a random iteration algorithm. An IFS with condensation consists of a complete metric space (X, d) together with a finite set of contraction mappings (transformations) $w_n: X \to X$, with contractivity factors s_n, for $n = 1, 2, \cdots, N$, and a condensation transformation w_0. The result of the IFS is called an attractor.

The following affine transformations were used in the IFS with condensation to generate the fractal trees. The condensation transformation was

$$w_0(x) = w_0\begin{pmatrix} x_1 \\ x_2 \end{pmatrix} = \begin{bmatrix} 0 & 0 \\ 0 & 0.447 \end{bmatrix}\begin{bmatrix} x_1 \\ x_2 \end{bmatrix} \tag{5}$$

and the contraction mappings were

$$w_1(x) = w_1\begin{pmatrix} x_1 \\ x_2 \end{pmatrix} = s_1\begin{bmatrix} \cos\theta & -\sin\theta \\ \sin\theta & \cos\theta \end{bmatrix}\begin{bmatrix} x_1 \\ x_2 \end{bmatrix} + \begin{bmatrix} e_1 \\ f_1 \end{bmatrix} \tag{6}$$

$$w_2(x) = w_2\begin{pmatrix} x_1 \\ x_2 \end{pmatrix} = s_2\begin{bmatrix} \cos\theta & \sin\theta \\ -\sin\theta & \cos\theta \end{bmatrix}\begin{bmatrix} x_1 \\ x_2 \end{bmatrix} + \begin{bmatrix} e_2 \\ f_2 \end{bmatrix} \tag{7}$$

The fractal tree shown in Figure 8*a* is the attractor of an IFS and was generated from a random iteration algorithm, while the fractal tree shown in Figure 8*b* was generated from a deterministic algorithm which allowed the network order to be set by the user. Both trees have the same values for the contractivity factors ($s_1 = s_2 = 0.6$), translation vectors ($(e_1, f_1) = (e_2, f_2) = (0, 0.5)$), and angle θ ($\theta = \pi/4$ radians).

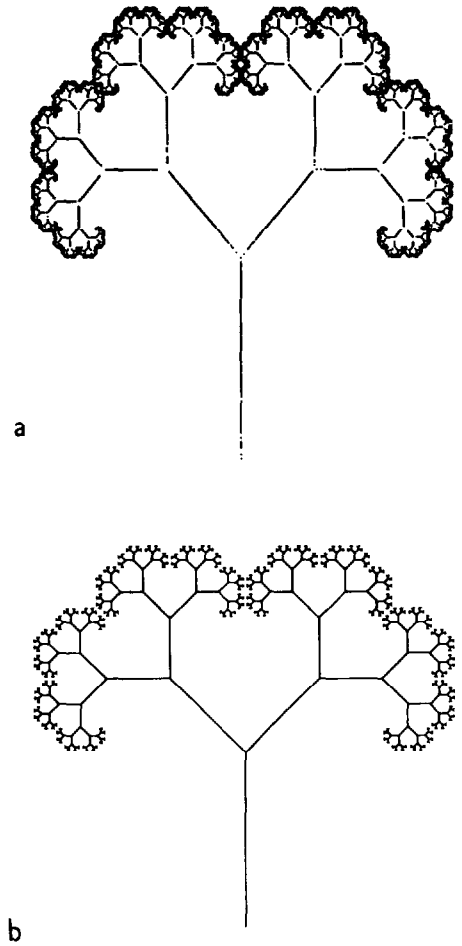

Fig. 8. Fractal trees generated with IFS. The fractal dimensions of both attractors are 1.36 ($R_B = 2$ and $R_L = 1.67$). The attractor corresponds to a river network (*a*) of large order where each stream is a set of points along a straight line, and (*b*) of order $\Omega = 10$ where each stream is a straight line.

For the case where the contraction mappings w_n are similitudes (such as those in (6) and (7)) with scaling factors s_n, *Barnsley* [1988] gives a solution for the fractal dimension for the attractor of a hyperbolic iterated function system as

$$\sum_{n=1}^{N} |s_n|^D = 1 \tag{8}$$

where D is the fractal dimension of the attractor of the IFS and N is the number of contraction mappings. Since this fractal dimension is equivalent to the box-counting dimension, the box-counting method can be used to determine its value.

The fractal dimension of a fractal tree where all contractivity factors are equal ($s_n = s$, for $n = 1, 2, \cdots, N$) is

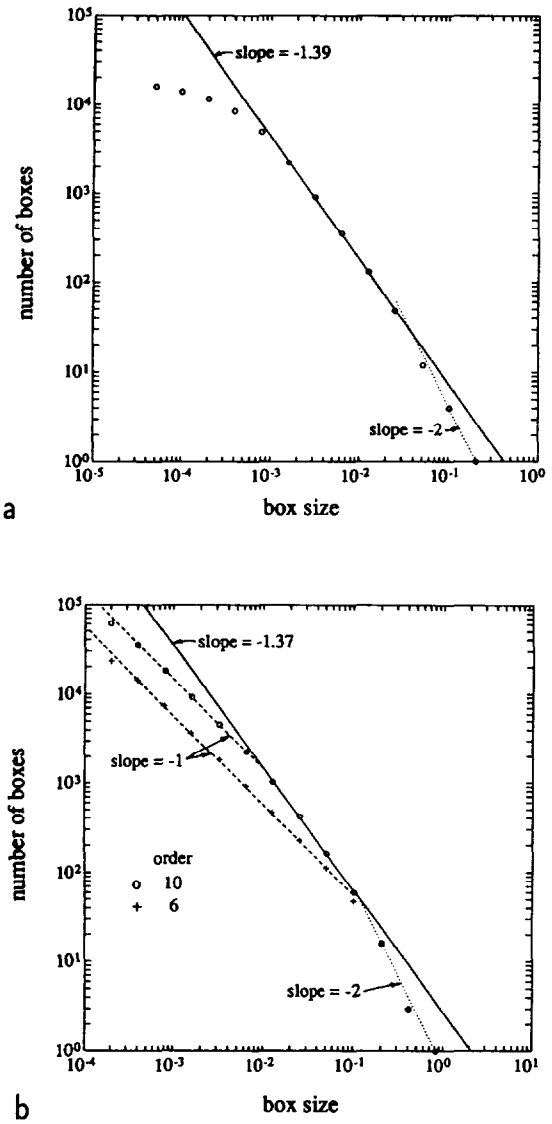

Fig. 9. Box-counting estimates of fractal dimension: (*a*) the attractor of Figure 8*a*, and (*b*) the attractor of Figure 8*b*.

$$D = \frac{\log (1/N)}{\log |s|} \tag{9}$$

The fractal dimension of both of the example trees is $D = 1.36$ since $N = 2$ and $s = 0.6$.

Having two contraction mappings ($N = 2$) is equivalent to having a bifurcation ratio of 2 in a channel network (that is, $R_B = N$). Since the two contractivity factors are equal, they can be related to the length ratio ($s_1 = s_2 = 1/R_L$). The fractal dimension of a tree can then be written as

$$D = \frac{\log R_B}{\log R_L} \tag{10}$$

which is the same result as that obtained by *LaBarbera and Rosso* [1989]. Since this dimension is equivalent to the box-counting dimension, the box-counting method can be used to estimate the value of the branching structure fractal dimension D_b in actual channel networks when estimates of R_B and R_L either do not exist or are not reliable.

The box-counting method was applied to the artificial channel networks shown in Figures 8*a* and 8*b* with the resulting fractal plots shown in Figures 9*a* and 9*b*, respectively. The artificial network in Figure 8*a* corresponds to a very large order network. The fractal plot for this network (Figure 9*a*) illustrates some problems associated with interpreting the results of the box-counting method. At the smallest box sizes the slope of the curve approaches zero, which indicates that at smaller box sizes each box contains a single point. At slightly larger box sizes there is a transition to the slope corresponding to the true fractal dimension. At the largest box sizes the slope will approach a slope of 2 because all the points are included in only a few boxes. These regions should be ignored because they are inherent in the fractal plot resulting from the box-counting method. Often these regions are not shown on the fractal plot. The intermediate range of box sizes on the plot clearly shows that the fractal dimension of the branching structure can be obtained from the slope of the box-counting fractal plot, which in this case is estimated to be 1.39.

The fractal plot in Figure 9*b* shows the results of the box-counting method for two artificial networks with network orders of 6 and 10. For these finite-order networks the smallest box sizes where the slope approaches zero do not exist. The intermediate box sizes which give valuable information show two distinct regions. One region (at small box sizes) shows a slope indicating the fractal dimension of individual streams. The slope of -1 here indicates that $D_s = 1$, which must be true since the individual streams were generated with straight lines. A second region (at larger box sizes) indicates the fractal dimension of the artificial network. Finally, the figure indicates that the region showing the fractal dimension of the network becomes smaller as the network order becomes smaller, and in fact it eventually disappears (as seen with the order 6 network). If the true fractal dimension was not known for the order 6 network, one could misinterpret the slope of 2 as indicating a space-filling network, whereas in fact, this is far from being the case since the true fractal dimension is 1.36. One should be aware of these estimation problems (mainly arising from applying asymptotic results to low-order networks) when interpretations are made on systems of unknown fractal dimensions.

3.2.2. *Actual channel networks.* Figures 10*a*–10*c* show the box-counting estimates of the fractal dimension of the South Fork Smith River, Schoharie Creek, and Big Creek channel networks, respectively. In general, two slopes will be seen on the fractal plots: (1) at small box sizes the slope indicates the fractal dimension of individual streams, and (2) at larger box sizes the slope gives the fractal dimension of the channel network D_{cn}. The box-counting estimates of the channel networks are found to be 1.79 for the South Fork Smith River, 1.75 for Schoharie Creek, and 1.76 for Big Creek. These estimates were obtained from the slope of the longest straight line segment (which corresponds to the smallest threshold area) in the fractal plots (Figures 10*a*–10*c*). Estimates from larger threshold areas would differ slightly simply because the number of points used in the estimation of the straight line segment of the curve would differ. Although the decision of how many points to include in the slope estimation is somewhat subjective, it is observed that the well-defined straight lines of slopes 1.79, 1.75, and 1.76 are consistent with all straight line segments that would

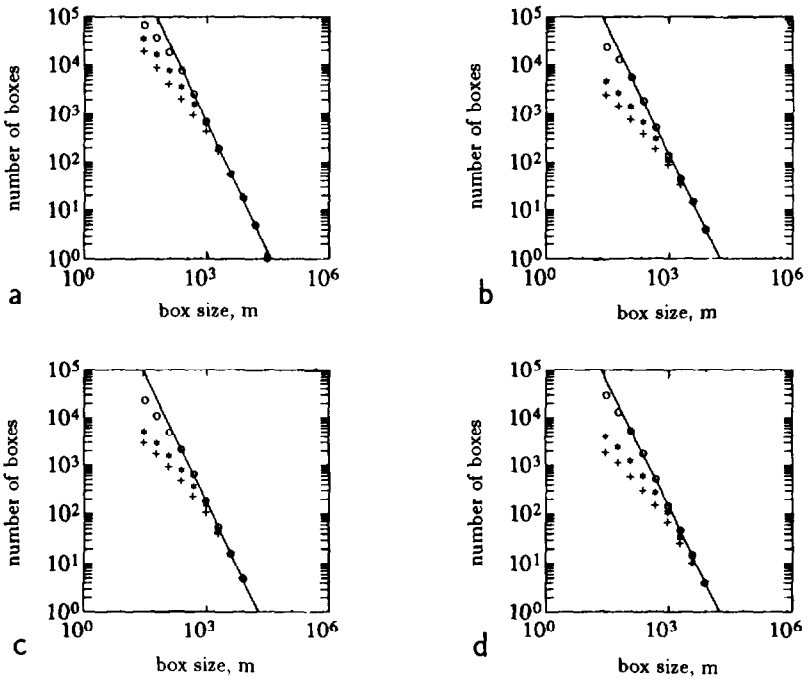

Fig. 10. The effect of threshold area on the box-counting estimate of the fractal dimension of the channel networks extracted from 30-m resolution DEM data. (*a*) South Fork Smith River, constant A_{th} (slope, −1.79; threshold areas: 0.0288 km^2 (circles), 0.2304 km^2 (asterisks), 0.9216 km^2 (pluses)); (*b*) Schoharie Creek, constant A_{th} (slope, −1.75; threshold areas: 0.0144 km^2 (circles), 0.2304 km^2 (asterisks), 0.9216 km^2 (pluses)); (*c*) Big Creek, constant A_{th} (slope, −1.76; threshold areas: 0.0144 km^2 (circles), 0.2304 km^2 (asterisks), 0.9216 km^2 (pluses)); (*d*) Schoharie Creek, slope-dependent $A_{th} = CS^{-2}$ (slope, −1.73; mean source areas: 0.0099 km^2 (circles), 0.2043 km^2 (asterisks), 1.2042 km^2 (pluses)).

have been obtained had larger threshold areas been used and thus we choose to report these as the box-counting estimates of the channel networks. Since the fractal dimension of individual streams was found to be almost 1 (0.99, 0.97, and 1.00, respectively) for these three networks (see Figure 11), the fractal dimension of the channel networks D_{cn} is approximately equal to the branching fractal dimension D_b. More specifically, using (1) the estimates of the fractal dimension of the branching structures are equal to 1.81, 1.80, and 1.76 for the South Fork Smith River, Schoharie Creek, and Big Creek, respectively.

A comparison of the box-counting estimates with Hortonian estimates of the fractal dimension of the branching structures reveals that there is a consistency between these two estimates, in that the box-counting estimates are within the range of the Hortonian estimates. For Schoharie Creek the box-counting estimate is equal to 1.80, which is the value of the only Hortonian estimate not greater than 2 (see Table 3). Our explanation of the greater than 2 fractal dimension estimates for this network is that for a watershed such as Schoharie Creek with uneven distribution of slopes (that is, different ranges and variability of slopes in different parts of the watershed) a constant critical support area for channel initiation is not appropriate but A_{th} depends on the local slope. In fact, when slope-dependent thresholds were used ($A_{th} = CS^{-2}$ for values of C given in Table 4) the estimates of R_B and R_L were such that $\log R_B/\log R_L$ was less than 2 for all except two thresholds. Moreover, the box-counting estimate of the branching structure which was now found to be 1.73 (see Figure 10*d*) was well within the range of the Hortonian estimates. For comparison to the constant threshold area case, the corresponding mean source area values for all C values are given in Table 4. It is seen that the C values chosen correspond to the same realistic range of constant threshold areas for channel initiation although the networks now look different. It is thus hypothesized that the need for a slope-dependent threshold for channel initiation (which has been argued both on empirical and theoretical grounds [e.g., *Montgomery and Dietrich*, 1988, 1993]) may be seen even from the more realistic Hortonian fractal dimension estimates obtained from the channel networks extracted with a slope-dependent A_{th} versus those extracted with constant A_{th}. Analysis of more channel networks and comparison

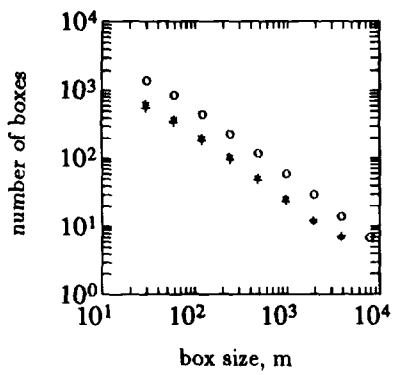

Fig. 11. Fractal plots for the mainstreams (extracted from 30-m resolution DEM data) of the South Fork Smith River (circles) with a threshold area of 0.4608 km^2 (D_s = 0.99), Schoharie Creek (pluses) with a threshold area of 0.6912 km^2 (D_s = 0.97), and Big Creek (asterisks) with a threshold area of 0.2304 km^2 (D_s = 1.00).

TABLE 4. Horton's Ratios for Networks Extracted From a 30-m Resolution DEM Using Slope-Dependent Threshold Areas $A_{th}S^2 = C$ for Schoharie Creek, New York

C, m^2	Mean Source Area, km^2	Basin Order (Ω)	Number of Streams	R_B	R_L	log R_B/ log R_L
2,000	0.0171	6	2452	4.22 (−0.999)	1.87 (0.988)	2.31
4,000	0.0360	6	1118	4.13 (−0.999)	1.95 (0.991)	2.12
6,000	0.0594	5	661	4.21 (−0.999)	2.21 (0.990)	1.81
8,000	0.0864	5	453	4.04 (−0.999)	2.15 (0.986)	1.82
12,000	0.1296	5	269	3.84 (−0.999)	2.12 (0.993)	1.79
16,000	0.2043	5	172	3.74 (−0.998)	2.08 (0.987)	1.80
24,000	0.2907	4	101	3.80 (−0.998)	2.36 (0.979)	1.55
32,000	0.4518	4	74	3.52 (−0.999)	1.96 (0.940)	1.87
64,000	1.2042	3	30	4.18 (−0.990)	2.30 (0.891)	1.71

Values in parentheses are the coefficients of correlation R of the weighted least squares regression.

with field-mapped channel networks are needed to substantiate or disprove the above hypothesis.

4. Resolution of DEM Data

All of the above results were obtained from channel networks extracted from 30 by 30 m DEM data. Sometimes such data are not available, and lower resolution data, for example, 60 by 60 m data, must be used. In order to investigate the effects of the DEM data resolution on estimates of R_B, R_L, and D_b, lower-resolution DEM data sets were obtained by filtering (averaging) the original 30 by 30 m data. This operation is reasonable under the assumption that digital elevation data at a given resolution (grid size) can be interpreted as averages over an area surrounding the point at which elevation is reported. The filtering kernel used is based on orthogonal wavelet transforms and more specifically on the D4 wavelet [*Strang*, 1989]. Wavelet transforms provide a generalized framework for multiscale (multiresolution) analysis. This framework extends the usual method of averaging adjacent pixels to go from one resolution to another. The use of the D4 wavelet (which has two vanishing moments) provides a better frequency localization as compared to the method of simple averaging. Filtering using wavelets provides localization both in space and frequency, and thus smoothing is obtained based on the neighboring values (24 surrounding values in the case of the D4 wavelet) only and not on all features of the terrain as a Fourier transform–based filtering would provide. This filter also provides estimated fields which are consistent at all scales and, because sampling is done uniformly on a logarithmic scale, it resembles most closely the smoothing procedure that the eye of a cartographer would apply in degrading the resolution of a map [*Mallat*, 1989, p. 2093]. Other advantages of wavelet transforms for multiresolution analysis of hydrologic processes are extensively discussed by *Kumar and Foufoula-Georgiou* [this issue].

Table 5 shows the effect of changing resolution on estimates of R_B, R_L, and $D_b = \log R_B/\log R_L$ for different threshold areas in two of the watersheds. In general, it is observed that for a given threshold area the variability of estimates due to resolution is of the same order of magnitude (if not less) as that due to threshold area selection (compare with Table 3) apart from very low resolutions where some abrupt changes are observed. Although one might criticize the "artificial" way by which lower-resolution data were created, the use of varying resolution maps and corresponding channel networks is subject to the risk of introducing into the analysis the subjectivity of the cartographer interpreting the terrain from lower-resolution maps. Our analysis is by no means complete, and simultaneous use of generated and actual varying resolution data should be used to better address the problem of the sensitivity of scaling parameter estimates on the resolution of the DEM data. At this point we only offer a recommendation that every effort should be made to address and resolve several estimation problems before the need for higher-resolution data can be justified for estimation of scaling properties of channel networks. Although high-resolution data are no doubt needed for identification of the channel initiation scale, they may not be needed for estimation of scaling properties if one considers (even with higher-resolution data) the significant variability of the estimates due to arbitrarily specified threshold areas.

5. Concluding Remarks

Morphometric properties (such as drainage density, length of drainage paths, and external and internal links) and scaling properties (such as Horton's ratios and fractal dimension) of a channel network are thought of as being characteristic descriptors of a landscape. The usefulness of these properties in hydrologic studies has stimulated their estimation from DEM data where a channel network is usually extracted automatically based on a prespecified critical support or threshold area A_{th} which indicates the minimum area required to drain to a point for a channel to form.

Several attempts have been made to predict the most appropriate threshold area in the sense that by using that value the extracted channel network will resemble the one that would be observed in the field. In our opinion these efforts have not met with success, and the problem of defining the channel initiation scale is still an open problem. Until this problem is resolved, researchers and practitioners will continue to use arbitrary threshold areas for channel network extraction from DEM data.

In this paper we have reported the results of a study which aimed at quantifying the effects of threshold area selection on the estimation of morphometric and scaling properties of a channel network. The results indicate that the threshold area considerably affects the estimation of morphometric properties to the point that reporting these values without reference to the threshold area used is meaningless. As far as

TABLE 5. Horton's Ratios for Networks Extracted From DEM Resolutions (Grid Sizes) Greater Than 30 m

Grid Size, m	Threshold Area: Area, km^2	Threshold Area: Number of Pixels	Basin Order (Ω)	Number of Streams	R_B	R_L	log R_B/ log R_L
			South Fork Smith River, California				
60	0.0576	16	7	3533	4.39 (−0.999)	2.16 (0.997)	1.92
120		4	6	4425	4.96 (−0.999)	2.29 (0.998)	1.93
60	0.1152	32	6	1677	4.37 (−0.999)	2.23 (0.999)	1.84
120		8	6	1756	4.68 (−0.999)	2.25 (0.998)	1.91
240		2	6	2696	5.09 (−0.999)	2.16 (0.996)	2.12
60	0.2304	64	6	811	4.27 (−0.998)	2.12 (0.987)	1.93
120		16	6	811	4.31 (−0.998)	2.05 (0.990)	2.03
240		4	6	958	4.42 (−0.998)	2.19 (0.998)	1.90
60	0.3456	96	6	567	3.88 (−0.997)	2.02 (0.986)	1.93
120		24	5	553	4.79 (−0.999)	2.46 (0.998)	1.74
240		6	5	586	4.69 (−0.999)	2.39 (0.999)	1.78
60	0.4032	112	5	488	4.53 (−0.999)	2.49 (0.999)	1.66
120		28	5	472	5.18 (−0.999)	2.44 (0.977)	1.85
240		7	5	493	4.63 (−0.999)	2.38 (0.999)	1.76
60	0.4608	128	5	429	4.36 (−0.999)	2.40 (0.999)	1.68
120		32	5	423	5.00 (−0.999)	2.42 (0.976)	1.82
240		8	5	418	4.55 (−0.999)	2.29 (0.994)	1.83
480		2	5	614	4.96 (−0.997)	2.34 (0.996)	1.88
60	0.6912	192	5	301	4.01 (−0.999)	2.24 (0.995)	1.73
120		48	5	287	4.36 (−0.998)	2.23 (0.974)	1.84
240		12	5	275	3.90 (−0.998)	2.12 (0.993)	1.81
480		3	5	341	4.83 (−0.997)	2.22 (0.976)	1.98
60	0.9216	256	5	211	3.95 (−0.998)	2.10 (0.969)	1.86
120		64	5	204	3.97 (−0.998)	2.05 (0.968)	1.92
240		16	5	213	3.92 (−0.998)	2.04 (0.971)	1.91
480		4	4	224	5.19 (−0.999)	2.90 (0.993)	1.55
			Schoharie Creek, New York				
60	0.0288	8	6	1694	4.56 (−0.999)	2.03 (0.999)	2.14
120		2	6	1924	4.66 (−0.999)	1.85 (0.993)	2.51
60	0.0576	16	6	780	4.15 (−0.999)	1.96 (0.997)	2.11
120		4	6	905	4.34 (−0.998)	1.85 (0.987)	2.40
60	0.1152	32	5	386	4.49 (−0.999)	2.30 (0.999)	1.81
120		8	5	409	4.58 (−0.999)	2.19 (0.999)	1.94
240		2	5	499	4.88 (−0.999)	1.95 (0.992)	2.37
60	0.2304	64	4	167	5.12 (−0.999)	2.43 (0.986)	1.84
120		16	4	175	5.63 (−0.997)	2.64 (0.999)	1.78
240		4	5	214	4.16 (−0.997)	1.88 (0.997)	2.26
60	0.4608	128	4	93	4.76 (−0.996)	2.45 (0.998)	1.74
120		32	4	88	4.55 (−0.995)	2.28 (0.998)	1.84
240		8	4	94	4.67 (−0.995)	2.33 (0.995)	1.82
480		2	4	129	5.01 (−0.999)	2.14 (0.988)	2.12
60	0.6912	192	4	61	4.02 (−0.996)	2.02 (0.997)	1.97
120		48	4	59	4.01 (−0.995)	1.97 (0.997)	2.05
240		12	4	56	3.82 (−0.996)	1.99 (0.997)	1.95
480		3	4	74	4.56 (−0.994)	1.89 (0.996)	2.38
60	0.9216	256	4	44	3.51 (−0.995)	1.76 (0.980)	2.22
120		64	4	47	3.65 (−0.995)	1.82 (0.975)	2.17
240		16	4	44	3.58 (−0.993)	1.84 (0.961)	2.10
480		4	3	50	6.32 (−0.999)	2.74 (0.984)	1.83

Values in parentheses are the coefficients of correlation R of the weighted least squares regression.

estimation of scaling properties is concerned, the results indicate that the variability, due to threshold area selection, of Horton's ratios and the fractal dimensions estimated from them is significant (a range of approximately 0.2–0.3 for the networks analyzed) even if incomplete channel networks (which were found to occur unpredictably at some threshold areas) are detected and excluded from the analysis. Care also must be exercised in resolving the issue of constant versus slope-dependent A_{th} for channel network extraction. For one of the basins we examined, which had uneven distribution of slopes, the channel network extracted with constant A_{th} areas resulted in unrealistic (greater than 2) fractal dimension estimates. This was interpreted as pointing out the need for a slope-dependent A_{th} for which, indeed, more realistic estimates were obtained.

Since DEM data are anticipated to see increased use over the next several years, efforts should be directed to resolving the problem of channel initiation scale so that networks close to the true channel networks can be extracted from DEM data for hydrologic studies. More field studies such as those of *Montgomery and Dietrich* [1988] should be performed to create a data base for testing the theories of channel initia-

tion scale. In the meanwhile, however, users of DEM data should be aware of the existing estimation problems, some of which were pointed out by our analysis.

Acknowledgments. This research was supported in part by the Minnesota Water Resources Research Center grant USDI-14-08-0001-G1570-02 and NSF grant CES-8957469. Computational resources were provided in part by the Minnesota Supercomputer Institute. We thank David Tarboton for providing us the DEM data used in our analysis as well as his programs for channel network extraction.

REFERENCES

Andah, K., F. Siccardi, and P. LaBarbera, Is a drainage network from a digital terrain model a model for the real network? (abstract), *Eos Trans. AGU*, *68*(44), 1272, 1987.

Band, L. E., Topographic partition of watersheds with digital elevation models, *Water Resour. Res.*, *22*(1), 15–24, 1986.

Band, L. E., A terrain-based watershed information system, *Hydrol. Processes*, *4*, 151–162, 1989.

Barnsley, M., *Fractals Everywhere*, Academic, San Diego, Calif., 1988.

Carlston, C. W., Drainage density and streamflow: Physiographic and hydraulic studies of rivers, *U.S. Geol. Surv. Prof. Pap.*, *422-c*, 1963.

Chorowicz, J., C. Ichoku, S. Riazanoff, Y.-J. Kim, and B. Cervelle, A combined algorithm for automated drainage network extraction, *Water Resour. Res.*, *28*(5), 1293–1302, 1992.

Coates, D. R., Quantitative geomorphology of small drainage basins of southern Indiana, *Tech. Rep. 10*, Dep. of Geol., Columbia Univ., New York, 1958.

Coffman, D. M., E. A. Keller, and W. N. Melhorn, New topologic relationship as an indicator of drainage network evolution, *Water Resour. Res.*, *8*(6), 1497–1505, 1972.

Eagleson, P. S., *Dynamic Hydrology*, McGraw-Hill, New York, 1970.

Fairfield, J., and P. Leymarie, Drainage networks from grid digital elevation models, *Water Resour. Res.*, *27*(5), 709–717, 1991. (Correction, *Water Resour. Res.*, *27*(10), 2809, 1991.)

Falconer, K., *Fractal Geometry: Mathematical Foundations and Applications*, John Wiley, New York, 1990.

Freeman, T. G., Calculating catchment area with divergent flow based on a regular grid, *Comput. Geosci.*, *17*(3), 413–422, 1991.

Gardner, T. W., K. C. Sasowsky, and R. L. Day, Automated extraction of geomorphic properties from digital elevation data, *Z. Geomorphol., Suppl. 80*, 57–68, 1991.

Gupta, V. K., E. Waymire, and C. Y. Wang, A representation of an instantaneous unit hydrograph from geomorphology, *Water Resour. Res.*, *16*(5), 855–862, 1980.

Helmlinger, K. R., and E. Foufoula-Georgiou, A geomorphologic study of river basins and hydrologic response, *Tech. Rep. 134*, Water Resour. Res. Center, Univ. of Minn., St. Paul, 1992.

Helmlinger, K., E. Foufoula-Georgiou, and D. Montgomery, On the prediction of hillslope scale from morphometric and climatic properties of a basin (abstract), *Eos Trans. AGU*, *73*(25), Western Pacific Geophysics Meeting suppl., 36, 1992.

Hjelmfelt, A. T., Jr., Fractals and the river-length catchment-area ratio, *Water Resour. Bull.*, *24*(2), 455–459, 1988.

Jenson, S. K., Methods and applications in surface depression analysis, paper presented at Auto-Carto 8, Baltimore, Md., 1987.

Jenson, S. K., and J. O. Domingue, Extracting topographic structure from digital elevation data for geographic information system analysis, *Photogramm. Eng. Remote Sens.*, *54*, 1593–1600, 1988.

Klinkenberg, B., and M. F. Goodchild, The fractal properties of topography: A comparison of methods, *Earth Surf. Processes Landforms*, *17*, 217–234, 1992.

Kumar, P., and E. Foufoula-Georgiou, A multicomponent decomposition of spatial rainfall fields, I, Segregation of large- and small-scale features using wavelet transforms, *Water Resour. Res.*, this issue.

LaBarbera, P., and R. Rosso, Fractal geometry of river networks (abstract), *Eos Trans. AGU*, *68*(44), 1276, 1987.

LaBarbera, P., and R. Rosso, On the fractal dimension of stream networks, *Water Resour. Res.*, *25*(4), 735–741, 1989.

LaBarbera, P., and R. Rosso, Reply, *Water Resour. Res.*, *26*(9), 2245–2248, 1990.

Lammers, R. B., and L. E. Band, Automatic object representation of drainage basins, *Comput. Geosci.*, *16*(6), 787–810, 1990.

Mallat, S., Multifrequency channel decomposition of images and wavelet models, *IEEE Trans. Acoust. Speech Signal Process.*, *37*(12), 2091–2110, 1989.

Marani, A., R. Rigon, and A. Rinaldo, A note on fractal channel networks, *Water Resour. Res.*, *27*(12), 3041–3049, 1991.

Mark, D. M., Network models in geomorphology, in *Modelling Geomorphological Systems*, edited by M. G. Anderson, chap. 4, John Wiley, New York, 1988.

Mark, D. M., and P. B. Aronson, Scale-dependent fractal dimensions of topographic surfaces: An empirical investigation, with applications in geomorphology and computer mapping, *Math. Geol.*, *16*(7), 671–683, 1984.

Martz, L. W., and E. deJong, CATCH: A FORTRAN program for measuring the catchment area from digital elevation models, *Comput. Geosci.*, *14*(5), 627–640, 1988.

Montgomery, D. R., and W. E. Dietrich, Where do channels begin?, *Nature*, *336*(6196), 232–234, 1988.

Montgomery, D. R., and W. E. Dietrich, Source areas, drainage density, and channel initiation, *Water Resour. Res.*, *25*(8), 1907–1918, 1989.

Montgomery, D. R., and W. E. Dietrich, Channel initiation and the problem of landscape scale, *Science*, *255*, 826–830, 1992.

Montgomery, D. R., and W. E. Dietrich, Landscape dissection and drainage area/slope thresholds, in *Theory in Geomorphology*, edited by M. J. Kirkby, John Wiley, New York, 1993.

Montgomery, D. R., and E. Foufoula-Georgiou, Channel network source representation using digital elevation models, *Water Resour. Res.*, in press, 1993.

Moore, I. D., R. B. Grayson, and A. R. Ladson, Digital terrain modelling: A review of hydrological, geomorphological and biological applications, *Hydrol. Processes*, *5*(1), 3–30, 1991.

Morisawa, M. E., Relation of quantitative geomorphology to stream flow in representative watersheds of the Appalachian plateau province, *Tech. Rep. 20*, Dep. of Geol., Columbia Univ., New York, 1959.

Morris, D. G., and R. G. Heerdegen, Automatically derived catchment boundaries and channel networks and their hydrological applications, *Geomorphology*, *1*, 131–141, 1988.

O'Callaghan, J. F., and D. M. Mark, The extraction of drainage networks from digital elevation data, *Comput. Vision Graphics Image Process.*, *28*, 323–344, 1984.

Qian, J., R. W. Ehrich, and J. B. Campbell, DNESYS—An expert system for automatic extraction of drainage networks from digital elevation data, *IEEE Trans. Geosci. Remote Sens.*, *28*(1), 29–44, 1990.

Quinn, P., K. Beven, P. Chevallier, and O. Planchon, The prediction of hillslope flow paths for distributed hydrological modelling using digital terrain models, *Hydrol. Processes*, *5*(1), 59–79, 1991.

Robert, A., and A. G. Roy, On the fractal interpretation of the mainstream length–drainage area relationship, *Water Resour. Res.*, *26*(5), 839–842, 1990.

Rodriguez-Iturbe, I., and J. B. Valdes, The geomorphologic structure of hydrologic response, *Water Resour. Res.*, *15*(6), 1409–1420, 1979.

Rosso, R., Nash model relation to Horton order ratios, *Water Resour. Res.*, *20*(7), 914–920, 1984.

Rosso, R., B. Bacchi, and P. LaBarbera, Fractal relation of mainstream length to catchment area in river networks, *Water Resour. Res.*, *27*(3), 381–387, 1991.

Seemuller, W. W., The extraction of ordered vector drainage networks from elevation data, *Comput. Vision Graphics Image Process.*, *47*, 45–58, 1989.

Smart, J. S., Quantitative characterization of channel network structure, *Water Resour. Res.*, *8*(6), 1487–1496, 1972.

Smith, T. R., and F. P. Bretherton, Stability and the conservation of mass in drainage basin evolution, *Water Resour. Res.*, *8*(6), 1506–1529, 1972.

Strahler, A. N., Hypsometric (area-altitude) analysis of erosional topography, *Geol. Soc. Am. Bull.*, *63*, 1117–1142, 1952.

Strang, G., Wavelets and dilation equations: A brief introduction, *SIAM Rev.*, *31*(4), 614–627, 1989.

Tarboton, D. G., R. L. Bras, and I. Rodriguez-Iturbe, The fractal

nature of river networks, *Water Resour. Res.*, *24*(8), 1317–1322, 1988.

Tarboton, D. G., R. L. Bras, and I. Rodriguez-Iturbe, The analysis of river basins and channel networks using digital terrain data, *Tech. Rep. 326*, Ralph M. Parsons Lab. for Hydrol. and Water Resour. Syst., Dep. of Civ. Eng., Mass. Inst. of Technol., Cambridge, 1989.

Tarboton, D. G., R. L. Bras, and I. Rodriguez-Iturbe, Comment on "On the fractal dimension of stream networks" by P. LaBarbera and R. Rosso, *Water Resour. Res.*, *26*(9), 2243–2244, 1990.

Tarboton, D. G., R. L. Bras, and I. Rodriguez-Iturbe, On the extraction of channel networks from digital elevation data, *Hydrol. Processes*, *5*(1), 81–100, 1991.

Tribe, A. J., Automated recognition of valley heads from digital elevation models, *Earth Surf. Processes Landforms*, *16*, 33–49, 1991.

Tribe, A., Problems in automated recognition of valley features from digital elevation models and a new method toward their resolution, *Earth Surf. Processes Landforms*, *17*, 437–454, 1992.

U.S. Geological Survey, Digital elevation models: Data users guide, *Users Guide 5*, 38 pp., Natl. Mapp. Program, Reston, Va., 1987.

Yuan, L.-P., and N. L. Vanderpool, Drainage network simulation, *Comput. Geosci.*, *12*(5), 653–665, 1986.

E. Foufoula-Georgiou and K. R. Helmlinger, St. Anthony Falls Hydraulic Laboratory, Department of Civil and Mineral Engineering, The University of Minnesota-Twin Cities Campus, Mississippi River at Third Avenue, S. E., Minneapolis, MN 55414-2196.

P. Kumar, USRA, Hydrologic Sciences Branch, Laboratory for Hydrospheric Processes, Code 974, Building 22, NASA Goddard Space Flight Center, Greenbelt, MD 20771.

(Received July 22, 1992;
revised January 27, 1993;
accepted March 3, 1993.)